Biointerface Research in Applied Chemistry
Open-Access Journal (ISSN: 2069-5837)

Article
Volume 13, Issue 6, 2023, 556
https://doi.org/10.33263/BRIAC136.556

QSPR Model Through Revan Indices to Predict Physicochemically and ADMET Properties of Anti-Flaviviral Drugs to Treat Zika Virus

William Tamilarasi [1], Bommahalli Jayaraman Balamurugan [1,*]

[1] Division of Mathematics, School of Advanced Sciences, Vellore Institute of Technology, Chennai Campus, Vandalur-Kelambakkam road, Chennai-600127, Tamil Nadu, India; tamilarasi.w2019@vitstudent.ac.in (W.T.);
* Correspondence: balamurugan.bj@vit.ac.in (B.J.B.);

Scopus Author ID 57211566319
Received: 28.10.2022; Accepted: 20.01.2023; Published: 24.02.2023

Abstract: In chemical graph theory, a topological index is a tool that converts a chemical structure into a real number used to predict a molecule's various physical and chemical properties. It finds application in QSPR/QSAR investigations, quantum chemistry, and stereochemistry in drug discovery and pharmacology. The Zika virus (ZIKV), a flavivirus spread by Aedes mosquitoes, has evolved into a human menace that has become a global health crisis. Because there is no specific vaccination or treatment for ZIKV infection, the disease is treated with repurposed anti-flaviviral medications such as Mefloquine, Sertraline, Niclosamide, Tizoxanide, PHA-690509, Ribavirin, Emricasan, and Sofosbuvir. This article predicted the physicochemical and pharmacokinetic properties (ADMET) of the anti-flaviviral drugs using the QSPR model based on several Revan indices. The cubic regression model was used to analyze the relationships between these properties and indices. Further, some of the best predictive topological indices for the physicochemical and pharmacokinetic characteristics of anti-flaviviral therapies are identified, which will help the pharmaceutical and biotherapeutic industries to create new ZIKV capsules, medications, and vaccines.

Keywords: Revan indices; QSPR analysis; ADMET property; anti-flaviviral drugs.

1. Introduction

The Zika virus is a mosquito-borne disease of the Flavivirus genus, transmitted by Aedes mosquitoes that bite during the day. ZIKV was first observed in monkeys in Uganda in 1947. Later it was identified in humans in 1952 in Uganda and the United Republic of Tanzania. The most recent ZIKV outbreak in the Americas gained significant public attention since Zika infection can result in newborn babies' microcephaly and Guillain-Barre syndrome in adults. In [1], a descriptive analysis of Zika virus disease was conducted and reported that females and young adults have a higher cumulative incidence of Zika virus than males and neurological complications in adults. Moreover, some clinical similarities and relationships are found in Africa between the Zika virus and COVID-19 pandemic [2]. Since there are no approved vaccines or specific therapeutics to prevent or treat ZIKV infection, in [3], J. Devillers identified some potential repurposed and FDA-approved drugs like Mefloquine, Sertraline, Niclosamide, Tizoxanide, PHA-690509, Ribavirin, Emricasan, and Sofosbuvir that are used against ZIKV infection.

Mathematical models of chemical activities are combined with graph theory in the field of mathematical chemistry, known as chemical graph theory. In chemical graph theory, a topological index is a molecular descriptor that provides a mathematical formula to any graph that describes a molecular structure. The indices analyze the numerical values and explore a molecule's various physical and chemical features. Therefore, it is a practical means of avoiding expensive and time-consuming laboratory tests. In mathematical chemistry, molecular descriptors are important in quantitative structure-property relationship (QSPR) and quantitative structure-activity relationship (QSAR) studies. Topological indices are used to determine chemical compounds' chemical and physical properties, including boiling point, polarizability, entropy, enthalpy of vaporization, molar volume, refraction, etc. Several topological indices are based on degree, distance, spectrum, eccentricity, and matching. The Weiner index, defined by Harold Weiner in 1947 [4], is the most well-known and extensively used distance-based topological to compare the boiling point of several alkane isomers. The Zagreb index is a degree-based topological index defined by Gutman and Trinajstic [5], to investigate the correlation between the total $\boldsymbol{\pi}$-electron energy and molecular structure. The Estrada index [6] is based on the spectrum of the graph and is used in modeling the 3D structure of organic molecules. Currently, chemical data stores have registered more than 3000 topological indices. In QSPR and QSAR analysis of COVID-19 drugs, degree-based topological indices play a significant role [7-24]. In this article, we consider Revan indices based on Revan vertex degree to perform QSPR analysis which was defined by V. R. Kulli in [25].

Artificial intelligence, machine learning, and mathematical models have been used in drug discovery in recent years, which facilitate a new pathway in the history of pharmaceutical development. The physical and chemical characteristics, such as flash point, polar surface area, enthalpy, etc., and pharmaco-kinetic characteristics, such as absorption, distribution, metabolism, excretion, and toxicity (ADMET), are crucial in the design of pharmaceutical drugs. Finding and developing new drugs takes a lot of time, effort, and resources because the process is laborious and complex. Pharmacokinetics, a subfield of pharmacology, is the study that explains how medicine interacts with the body. Studying a drug's ADMET characteristics is essential for drug development and discovery. Pharmacokinetic studies examine the drug's rate of absorption, distribution within the body, rate of metabolization, rate of elimination from the body, and whether the drug has any harmful effects on organs or systems. The QSPR/QSAR modeling is one of the most important methods to correlate a chemical compound's molecular structure to various physicochemical and ADMET properties, providing useful information for drug development. Recently in [26], the ADMET properties and QSPR analysis of drugs against the Omicron variant of COVID-19 disease with some degree-based topological indices via M-polynomial were investigated.

Recently many researchers have been working on different topological indices for various antiviral, anticancer, COVID-19, antituberculosis, and asthma drugs to establish QSPR models with linear, quadratic, and cubic regression analyses between physicochemical properties of the drugs and topological indices. In [27], Havare examined the QSPR study utilizing curvilinear regression models for COVID-19 drugs and found that cubic regression models offer the most accurate assessment of the physicochemical characteristics of antiviral drugs used to treat COVID-19 patients. These works motivate us to study QSPR models of anti-flaviviral drugs for treating the Zika virus using the cubic regression method.

2. Materials and Methods

Let G be a connected graph with the vertex set $V(G)$ and edge set $E(G)$. The degree of a vertex u given by $d_G(u)$ is the number of vertices adjacent at u. The maximum and minimum degree of a graph G is given as $\Delta(G)$ and $\delta(G)$, respectively. The Revan vertex degree of a vertex $u \in G$ is defined as $r_G(u) = \Delta(G) + \delta(G) - d_G(u)$.The edge uv denotes the Revan edge connecting the Revan vertices u and v. A molecular graph is a graph-theoretical depiction of the chemical structure of a compound, where the vertices are the atoms of the molecule and the edges are chemical bonds between the atoms, with double bonds being considered parallel edges.

The Revan indices are defined as follows:

The first and second Revan indices [25] of a graph G is defined as

$R_1(G) = \sum_{uv \in E(G)}[r_G(u) + r_G(v)]$, $R_2(G) = \sum_{uv \in E(G)} r_G(u) r_G(v)$

The first and second hyper Revan indices [28] of a graph G is defined as

$HR_1(G) = \sum_{uv \in E(G)}[r_G(u) + r_G(v)]^2$, $HR_2(G) = \sum_{uv \in E(G)}[r_G(u) r_G(v)]^2$

The modified first and second Revan indices [29] of a graph G is defined as

${}^mR_1(G) = \sum_{uv \in E(G)} \frac{1}{r_G(u)+r_G(v)}$, ${}^mR_2(G) = \sum_{uv \in E(G)} \frac{1}{r_G(u) r_G(v)}$

The sum connectivity Revan index [30] of a graph G is defined as

$$SR(G) = \sum_{uv \in E(G)} \frac{1}{\sqrt{r_G(u) + r_G(v)}}$$

The product connectivity Revan index [31] of a graph G is defined as

$$PR(G) = \sum_{uv \in E(G)} \frac{1}{\sqrt{r_G(u) r_G(v)}}$$

The F-Revan index [32] of a graph G is defined as

$$FR(G) = \sum_{uv \in E(G)} [r_G(u)^2 + r_G(v)^2]$$

The Atom-Bond connectivity Revan index [33] of a graph G is defined as

$$ABCR(G) = \sum_{uv \in E(G)} \sqrt{\frac{r_G(u) + r_G(v) - 2}{r_G(u) r_G(v)}}$$

The Geometric-Arithmetic Revan index [33] of a graph G is defined as

$$GAR(G) = \sum_{uv \in E(G)} \frac{2\sqrt{r_G(u) r_G(v)}}{r_G(u) + r_G(v)}$$

The Harmonic Revan index [33] of a graph G is defined as

$$HR(G) = \sum_{uv \in E(G)} \frac{2}{r_G(u) + r_G(v)}$$

The Symmetric Division Revan index [33] of a graph G is defined as

$$SDR(G) = \sum_{uv \in E(G)} \frac{r_G(u)}{r_G(v)} + \frac{r_G(v)}{r_G(u)}$$

The anti-flaviviral drugs considered in this paper to treat Zika virus are Mefloquine, Sertraline, Niclosamide, Tizoxanide, PHA-690509, Ribavirin, Emricasan, and Sofosbuvir. The chemical structure and molecular graph of these drugs are depicted in Figure 1-8, whose QSPR analysis is carried out in this article.

2.1. Computation of Revan indices:

Using the Revan edge partition method and indices formulae, the values of various Revan indices for the molecular graphs of anti-flaviviral drugs are obtained in the following theorem. Tables 1–8 list the Revan edge partitioning of anti-flaviviral drugs. The chemical structures are drawn using the ChemDraw tool.

Theorem 1: The Revan indices for the molecular graph M of Mefloquine are as follows: $R_1(M) = 136$, $HR_1(M) = 608$, SR(M) =17.8449 , ${}^mR_1(M)$ =10.9428, $R_2(M) = 134$, $HR_2(M) = 780$, PR(M) =20.4380 , ${}^mR_2(M)$ =13.7916, FR(M) =340 , ABCR(M)=21.2666 , GAR(M) =32.0998, HR(M) =21.8857 , SDR(M)=87.5833.

Proof: From the molecular graph of Mefloquine in Figure 1(b), the Revan edge partitions are obtained and shown in Table 1, and by applying the above definitions of Revan indices, the computation of indices is obtained as follows.

(a) (b)

Figure 1. (a) Chemical structure and **(b)** molecular graph of Mefloquine.

Table 1. Revan edge partitioning of the molecular graph of Mefloquine.

$(r_G(u), r_G(v))/\ uv \in E(G)$	(4,3)	(4,2)	(4,1)	(3,3)	(3,2)	(3,1)	(2,2)	(2,1)	(1,1)
No. of edges	1	1	6	3	3	1	5	10	5

Now by using the above edge partition and indices formula, we get,

$R_1(M) = \sum_{uv\in E(M)}[r_M(u) + r_M(v)]$

= 1(4+3) +1(4+2) +6(4+1) +3(3+3) +3(3+2) + 5(2+2) + 10(2+1) + 5(1+1)

= 7+6+30+18+15+20+30+10

= 136

$R_2(M) = \sum_{uv\in E(M)} r_M(u)r_M(v)$

= 1(4×3) +1(4×2) +6(4×1) +3(3×3) +3(3×2) + 5(2×2) + 10(2×1) + 5(1×1)

= 1(12) +1(8) + 6(4) + 3(9) +3(6) + 5(4) + 10(2) + 5(1)

= 134

$HR_1(M) = \sum_{uv\in E(M)}[r_M(u) + r_M(v)]^2$

$= 1(4+3)^2 + 1(4+2)^2 + 6(4+1)^2 + 3(3+3)^2 + 3(3+2)^2 + 5(2+2)^2 + 10(2+1)^2 + 5(1+1)^2$

= 49 +36 +150 +108 +75 +80 +90 +20

= 608

$HR_2(M) = \sum_{uv\in E(M)}[r_M(u)r_M(v)]^2$

$= 1(4\times 3)^2 + 1(4\times 2)^2 + 6(4\times 1)^2 + 3(3\times 3)^2 + 3(3\times 2)^2 + 5(2\times 2)^2 + 10(2\times 1)^2 + 5(1\times 1)^2$

= 144 + 64 + 96 + 243 + 108 + 80 + 40 + 5

= 780

${}^mR_1(M) = \sum_{uv\in E(M)} \frac{1}{r_M(u)+r_M(v)}$

$= \frac{1}{7} + \frac{1}{6} + \frac{6}{5} + \frac{3}{6} + \frac{3}{5} + \frac{5}{2} + \frac{10}{3} + \frac{5}{2}$

= 10.9428

$$^{m}R_2(M) = \sum_{uv\in E(M)} \frac{1}{r_M(u)r_M(v)}$$
$$= \frac{1}{12} + \frac{1}{8} + \frac{6}{4} + \frac{3}{9} + \frac{3}{6} + \frac{5}{4} + \frac{10}{2} + \frac{5}{1}$$
$$= 13.7916$$

$$SR(M) = \sum_{uv\in E(M)} \frac{1}{\sqrt{r_M(u)+r_M(v)}}$$
$$= \frac{1}{\sqrt{7}} + \frac{1}{\sqrt{6}} + \frac{6}{\sqrt{5}} + \frac{3}{\sqrt{6}} + \frac{3}{\sqrt{5}} + \frac{5}{\sqrt{4}} + \frac{10}{\sqrt{3}} + \frac{5}{\sqrt{2}}$$
$$= 17.8449$$

$$PR(M) = \sum_{uv\in E(M)} \frac{1}{\sqrt{r_M(u)r_M(v)}}$$
$$= \frac{1}{\sqrt{12}} + \frac{1}{\sqrt{8}} + \frac{6}{2} + \frac{3}{3} + \frac{3}{\sqrt{6}} + \frac{5}{2} + \frac{10}{\sqrt{2}} + \frac{5}{1}$$
$$= 20.4380$$

$$FR(M) = \sum_{uv\in E(M)} [r_M(u)^2 + r_M(v)^2]$$
$$= 1(16+9) + 1(16+4) + 6(416+1) + 3(9+9) + 3(9+4) + 5(4+4) + 10(4+1) + 5(1+1)$$
$$= 25 + 20 + 102 + 54 + 39 + 40 + 50 + 10$$
$$= 340$$

$$ABCR(M) = \sum_{uv\in E(M)} \sqrt{\frac{r_M(u)+r_M(v)-2}{r_M(u)r_M(v)}}$$
$$= 1\sqrt{\frac{5}{12}} + 1\sqrt{\frac{4}{8}} + 6\sqrt{\frac{3}{4}} + 3\sqrt{\frac{4}{9}} + 3\sqrt{\frac{3}{6}} + 5\sqrt{\frac{2}{4}} + 10\sqrt{\frac{1}{2}}$$
$$= 21.2666$$

$$GAR(M) = \sum_{uv\in E(M)} \frac{2\sqrt{r_M(u)r_M(v)}}{r_M(u)+r_M(v)}$$
$$= 1\left(\frac{2\sqrt{12}}{7}\right) + 1\left(\frac{2\sqrt{8}}{6}\right) + 6\left(\frac{2\sqrt{4}}{5}\right) + 3\left(\frac{2\sqrt{9}}{6}\right) + 3\left(\frac{2\sqrt{6}}{5}\right) + 5\left(\frac{2\sqrt{4}}{4}\right) + 10\left(\frac{2\sqrt{2}}{3}\right) + 5\left(\frac{2\sqrt{1}}{2}\right)$$
$$= 32.0998$$

$$HR(M) = \sum_{uv\in E(M)} \frac{2}{r_M(u)+r_M(v)}$$
$$= 1\left(\frac{2}{7}\right) + 1\left(\frac{2}{6}\right) + 6\left(\frac{2}{5}\right) + 3\left(\frac{2}{6}\right) + 3\left(\frac{2}{5}\right) + 5\left(\frac{2}{2}\right) + 10\left(\frac{2}{3}\right) + 5\left(\frac{2}{2}\right)$$
$$= 21.8857$$

$$SDR(M) = \sum_{uv\in E(M)} \frac{r_M(u)}{r_M(v)} + \frac{r_M(v)}{r_M(u)}$$
$$= 1\left(\frac{4}{3} + \frac{3}{4}\right) + 1\left(\frac{4}{2} + \frac{2}{4}\right) + 6\left(\frac{4}{1} + \frac{1}{4}\right) + 3\left(\frac{3}{3} + \frac{3}{3}\right) + 3\left(\frac{3}{2} + \frac{2}{3}\right) + 5\left(\frac{2}{2} + \frac{2}{2}\right) +$$
$$10\left(\frac{2}{1} + \frac{1}{2}\right) + 5\left(\frac{1}{1} + \frac{1}{1}\right)$$
$$= 87.5833$$

Hence the theorem.

Similar to Theorem 1, the Revan indices for the chemical graphs of other drugs are computed in the following theorems by using their corresponding Revan edge partitions.

Theorem 2: The Revan indices for the molecular graph S of Sertraline is given by,

$R_1(S) = 108$, $HR_1(S) = 440$, $SR(S)$ =15.5631, $^{m}R_1(S)$ =8.55, $R_2(S) = 100$, $HR_2(S) = 476$, $PR(S)$ =17.8422, $^{m}R_2(S)$ =11.9444, $FR(S)$ =240, $ABCR(S)$=18.6619, $GAR(S)$ =27.7588, $HR(S)$ =17.1 , $SDR(S)$= 69.8333.

(a) (b)

Figure 2. (a) Chemical structure and **(b)** molecular graph of Sertraline.

Table 2. Revan edge partitioning of the molecular graph of Sertraline.

$(r_G(u), r_G(v))/\ uv \in E(G)$	(4,2)	(4,1)	(3,3)	(3,2)	(2,2)	(2,1)	(1,1)
No. of edges	2	2	1	2	7	12	3

Theorem 3: The Revan indices for the molecular graph N of Niclosamide is given by, $R_1(N) = 112$, $HR_1(N) = 436$, $SR(N)$ =17.7986, ${}^mR_1(N)$ =10.1595, $R_2(N) = 93$, $HR_2(N) = 419$, $PR(N)$ =21.5142, ${}^mR_2(N)$ =15.625, $FR(N)$ =250, $ABCR(N)$=19.3465, $GAR(N)$ =29.9763, $HR(N)$ =20.3190 , $SDR(N)$= 83.9999.

(a) (b)

Figure 3. Chemical structure **(a)** and molecular graph **(b)** of Niclosamide.

Table 3. Revan edge partitioning of the molecular graph of Niclosamide.

$(r_G(u), r_G(v))/\ uv \in E(G)$	(4,3)	(4,2)	(4,1)	(3,1)	(2,2)	(2,1)	(1,1)
No. of edges	1	1	3	5	4	12	6

Theorem 4: The Revan indices for the molecular graph T of Tizoxanide are given by, $R_1(T) = 106$, $HR_1(T) = 404$, $SR(T)$ =15.1282, ${}^mR_1(T)$ =8.3428, $R_2(T) = 88$, $HR_2(T) = 410$, $PR(T)$ =17.7526, ${}^mR_2(T)$ =12.0416, $FR(T)$ =228, $ABCR(T)$=18.5404, $GAR(T)$ =26.2226, $HR(T)$ =16.6857 , $SDR(T)$= 73.1666.

(a) (b)

Figure 4. **(a)** Chemical structure and**(b)** molecular graph of Tizoxanide.

Table 4. Revan edge partitioning of the molecular graph of Tizoxanide..

$(r_G(u), r_G(v))/\ uv \in E(G)$	(4,3)	(4,2)	(4,1)	(3,1)	(2,2)	(2,1)	(1,1)
No. of edges	1	1	1	7	5	10	3

Theorem 5: The Revan indices for the molecular graph P of PHA-690509 is given by, $R_1(P) = 126$, $HR_1(P) = 518$, $SR(P)$ =17.3034, ${}^mR_1(P)$ =9.2, $R_2(P) = 112$, $HR_2(P) = 522$, $PR(P)$ =19.7526, ${}^mR_2(P)$ =13.375, $FR(P)$ =294, $ABCR(P)$=24.1497, $GAR(P)$ =30.7379, $HR(P)$ =18.4 , $SDR(P)$= 87.25.

(a) (b)

Figure 5. (a) Chemical structure and**(b)** molecular graph of PHA-690509.

Table 5. Revan edge partitioning of the molecular graph of PHA-690509.

$(r_G(u), r_G(v))/\ uv \in E(G)$	(4,2)	(4,1)	(3,1)	(2,2)	(2,1)
No. of edges	5	1	6	4	17

Theorem 6: The Revan indices for the molecular graph R of Ribavirin is given by,

$R_1(R) = 114$, $HR_1(R) = 564$, $SR(R)$ =12.0953, ${}^mR_1(R)$ =5.9880, $R_2(R) = 135$, $HR_2(R) = 1005$, $PR(R)$ =12.3826, ${}^mR_2(R)$ =6.7777, $FR(R)$ =294, $ABCR(R)$=17.0115, $GAR(R)$ =24.2844, $HR(R)$ =11.9761 , $SDR(R)$=56.6666.

(a) (b)

Figure 6. (a) Chemical structure and **(b)** molecular graph of Ribavirin.

Table 6. Revan edge partitioning of the molecular graph of Ribavirin.

$(r_G(u), r_G(v))/\ uv \in E(G)$	(4,3)	(3,3)	(3,2)	(3,1)	(2,2)	(2,1)	(1,1)
No. of edges	4	1	5	3	8	3	1

Theorem 7: The Revan indices for the molecular graph E of Emricasan are given by,

$R_1(E) = 215$, $HR_1(E) = 911$, $SR(E)$ =29.8136, ${}^mR_1(E)$ =16.3595, $R_2(E) = 197$, $HR_2(E) = 975$, $PR(E)$ =35.4589, ${}^mR_2(E)$ =24.2777, $FR(E)$ =529, $ABCR(E)$=35.6664, $GAR(E)$ =51.8354, $HR(E)$ =32.7190 , $SDR(E)$= 153.9999.

(a) (b)

Figure 7. (a) Chemical structure and **(b)** molecular graph of Emricasan.

Table 7. Revan edge partitioning of the molecular graph of Emricasan.

$(r_G(u), r_G(v))/\ uv \in E(G)$	(4,3)	(4,2)	(4,1)	(3,3)	(3,2)	(3,1)	(2,2)	(2,1)	(1,1)
No. of edges	1	4	7	1	2	13	6	13	9

Theorem 8: The Revan indices for the molecular graph S of Sofosbuvir are given by,

$R_1(S) = 300$, $HR_1(S) = 1894$, SR(S) =20.0263, ${}^mR_1(S)$ =8.2444, $R_2(S) = 442$, $HR_2(S) = 4618$, PR(S) =17.3286, ${}^mR_2(S)$ =6.3958, FR(S) =1010, ABCR(S)=34.0164, GAR(S) =46.9972, HR(S) =16.4888 , SDR(S)= 117.5998.

Table 8. Revan edge partitioning of the molecular graph of Sofosbuvir.

$(r_G(u), r_G(v))/\ uv \in E(G)$	(5,4)	(5,3)	(5,2)	(4,4)	(4,3)	(4,2)	(4,1)	(3,3)	(3,2)	(3,1)
No. of edges	1	5	2	1	5	8	4	12	10	1

The above-calculated values of Revan indices are presented in Tables 9 and 10. The graphical representation of Zika virus drugs with Revan indices is represented in Figures 9 and 10.

(a) (b)

Figure 8. (a) Chemical structure and **(b)** molecular graph of Sofosbuvir

Table 9. The values of different Revan indices for the molecular graph of Zika virus drugs.

Drugs	R_1	HR_1	SR	$^mR_1$	R_2	HR_2	PR
Mefloquine	136	608	17.8449	10.9428	134	780	20.480
Sertraline	108	440	15.5631	8.55	100	476	17.8422
Niclosamide	112	436	17.7986	10.1595	93	419	21.5142
Tizoxanide	106	404	15.1282	8.3428	88	410	17.7526
PHA-690509	126	518	17.3034	9.2	112	522	19.7526
Ribavirin	114	564	12.0953	5.9880	135	1005	12.3826
Emricasan	215	911	29.8136	16.3595	197	975	35.4589
Sofosbuvir	300	1894	20.0263	8.2444	442	4618	17.3286

Table 10. The values of different Revan indices for the molecular graph of Zika virus drugs.

Drugs	$^mR_2$	FR	ABCR	GAR	HR	SDR
Mefloquine	13.7916	340	21.2666	32.0998	21.8857	87.5833
Sertraline	11.9444	240	18.6619	27.7588	17.1	69.8333
Niclosamide	15.625	250	19.3465	29.9763	20.3190	83.9999
Tizoxanide	12.0416	228	185404	26.2226	16.6857	73.1666
PHA-690509	13.375	294	24.1497	30.7379	18.4	87.25
Ribavirin	6.7777	294	17.0115	24.2844	11.9761	56.6666
Emricasan	24.2777	529	35.6664	51.8354	32.7190	153.9999
Sofosbuvir	6.3958	1010	34.0164	46.9972	16.4888	117.5998

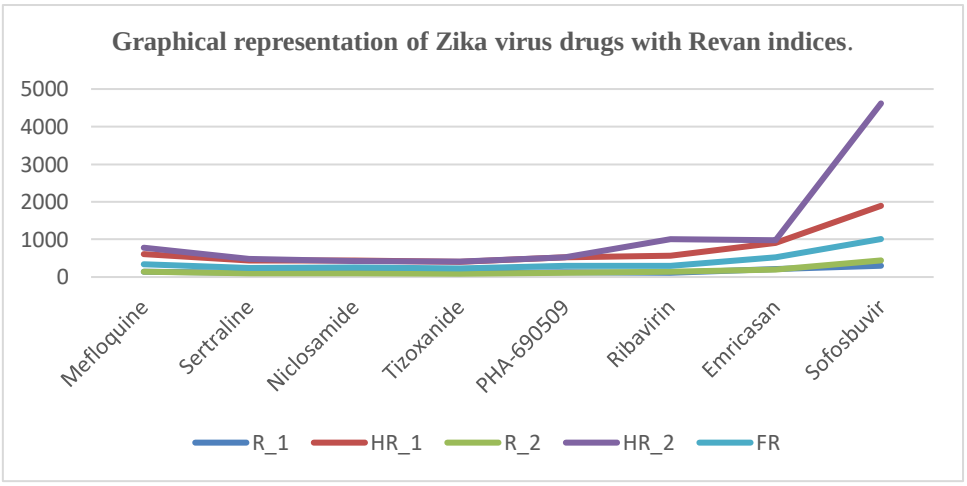

(a)

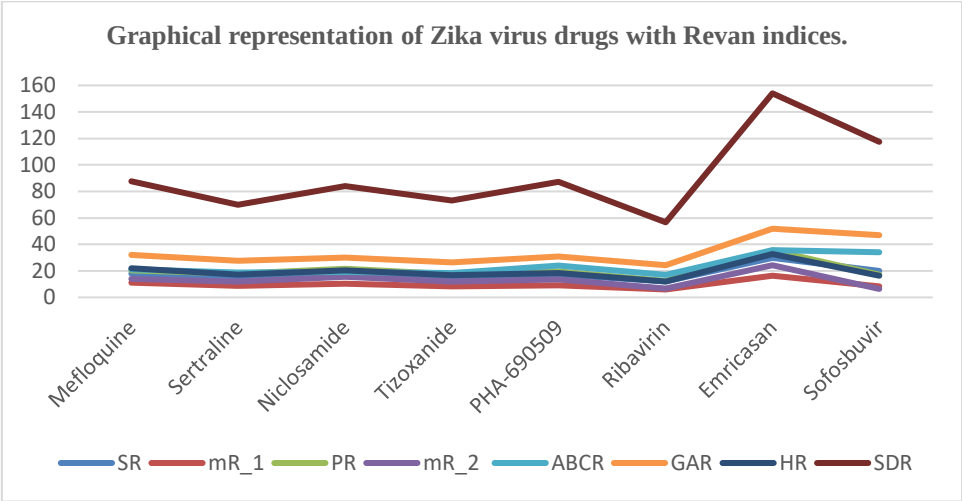

(b)

Figure 9. **(a)** and **(b)** Graphical representation of Zika virus drugs with various Revan indices.

3. Results and Discussion

3.1. QSPR model through Cubic regression analysis.

The cubic regression equation

$$P = A + B(RI) + C(RI)^2 + D(RI)^3 \quad (1)$$

is considered for the QSPR model to analyze the physicochemical and pharmacokinetic properties of drugs. In this equation, B, C, and D represent regression coefficients, RI represent Revan indices, and A is a constant. The cubic regression analysis is correlated for eight physicochemical and six pharmacokinetic (ADMET) properties values of the drugs with Revan indices values. Boiling point (BP), enthalpy of vaporization (EV), Flashpoint (FP), Molar refraction (MR), Polar surface area (PSA), Polarizability (P), Surface tension (ST), and Molar volume (MV) are the physicochemical properties considered in this study. The ADMET characteristics considered in this model are Intestinal Absorption (IA), CNS permeability (CNS), BBB permeability (BBB), Minnow Toxicity (MT), Total Clearance (TC), and Membrane permeability (Log P). The values of the physicochemical properties of the drugs given in Table 11 are obtained from https://www.chemspider.com, an online chemical structure database. Using the pkCSM platform, the ADMET properties of the drugs are predicted and listed in Table 14. Using SPSS program, the regression analyses are performed. Revan indices and the physicochemical characteristics of the aforementioned medications are correlated with each other, as shown in Table 12 by the cubic regression model. The statistical parameters for the cubic regression analysis with the highest correlation coefficient (R^2) value, minimal standard error (S. E), Max (R) value, maximum F-value, and p-value less than 0.05 are presented in Table 13, which are the factors for the goodness of fit. The results of the similar test for pharmacokinetic properties are shown in Tables 15 and 16. The cubic regression curve plot for the most reliable Revan indices for the physicochemical and pharmacokinetic characteristics of Zika virus medications is shown in Figures 10, 11, 12, 13, and 14.

Table 11. Physicochemical characteristics values of Zika virus drugs.

Drugs	BP	EV	FP	MR	PSA	P	ST	MV
Mefloquine	415.7	70.5	205.2	83	45	32.9	36.5	273.4
Sertraline	416.3	67	205.6	85.8	12	34	48.9	243.9
Niclosamide	424.5	70.5	210.5	79	95	31.3	71.7	202.5

Drugs	BP	EV	FP	MR	PSA	P	ST	MV
Tizoxanide	-	-	-	65.7	136	26.1	88.5	161.3
PHA-690509	-	-	-	94.3	96	37.4	47.7	271.6
Ribavirin	639.8	99.3	340.7	51.1	144	20.3	106.8	117.1
Emricasan	-	-	-	131	151	51.9	48.7	410.9
Sofosbuvir	-	-	-	123.5	163	48.9	58.7	374.6

Table 12. The correlation coefficient value (R^2) determined between Revan indices and the physicochemical characteristics values of Zika virus drugs.

Revan indices	BP	EV	FP	MR	PSA	P	ST	MV
R_1	0.604	0.645	0.604	0.805	0.294	0.800	0.264	0.824
HR_1	0.985	0.966	0.985	0.642	0.300	0.637	0.117	0.668
` SR	0.999	1	0.999	0.855	0.167	0.852	0.596	0.853
${}^mR_1$	0.984	0.980	0.984	0.460	0.357	0.459	0.632	0.501
R_2	0.383	0.475	0.383	0.562	0.304	0.558	0.071	0.585
HR_2	0.998	1	0.998	0.293	0.319	0.290	0.026	0.284
PR	0.999	0.991	0.999	0.497	0.299	0.496	0.562	0.504
${}^mR_2$	0.997	0.982	0.997	0.426	0.549	0.423	0.250	0.404
FR	0.923	0.953	0.923	0.707	0.297	0.702	0.162	0.732
$ABCR$	0.968	0.944	0.968	0.928	0.395	0.924	0.583	0.905
GAR	0.966	0.951	0.967	0.936	0.389	0.932	0.622	0.934
HR	0.984	0.980	0.984	0.460	0.357	0.459	0.632	0.501
SDR	0.978	0.978	0.979	0.914	0.491	0.909	0.599	0.896

Table 13. The statistical parameters for the cubic regression model having the highest correlation coefficient value (R^2) for various Revan indices with physicochemical properties of Zika virus drugs.

Cubic model	R	F	S. E	P
BP=6.02E4-1.19E4(SR)+7.79E2$(SR)^2$-16.86$(SR)^3$	0.999	360.096	7.129	0.037
EV=2.08E3-3.69E2(SR)+22.41$(SR)^2$-0.45$(SR)^3$	1	934.900	0.191	0.007
FP=3.62E4-7.14E3(SR)+4.68E2$(SR)^2$-10.15$(SR)^3$	0.999	362.909	4.294	0.037
EV=1.32E2-0.21 (HR_2)+1.5E-4$(HR_2)^2$+3.11E-8$(HR_2)^3$	1	1507.971	0.475	0.018
BP=3.63E3-4.47E2(PR)+20.39$(PR)^2$-0.3$(PR)^3$	1	623.704	5.420	0.028
FP=2.15E3-2.7E2(PR)+12.32$(PR)^2$-0.18$(PR)^3$	1	624.581	3.274	0.028
MR=-3.35E2+28.39(GAR)-0.63$(GAR)^2$+4.87E-3$(GAR)^3$	0.967	36.330	8.115	0.001
P=-1.34E2+11.38(GAR)-0.25$(GAR)^2$+1.97E-3$(GAR)^3$	0.965	34.057	3.304	0.001
MV=-3.01E3+3.68E2($ABCR$)13.7$(ABCR)^2$+0.17$(ABCR)^3$	0.951	23.871	36.397	0.003

Table 14. Pharmacokinetic properties (ADMET) values of Zika virus drugs.

Drugs	Intestinal absorption	CNS permeability	BBB permeability	Minnow Toxicity	Total clearance	LogP
Mefloquine	85.961	-2.675	0.488	0.913	0.43	4.4479
Sertraline	91.075	-1.094	0.596	0.39	0.917	5.1796
Niclosamide	87.083	-2.003	-0.598	1.423	0.213	3.8595
Tizoxanide	83.742	-2.477	-0.716	2.156	0.045	2.0092
PHA-690509	90.493	-2.1	-0.138	0.761	-0.065	3.9671
Ribavirin	54.988	-3.756	-0.921	4.626	0.623	-3.0115
Emricasan	31.042	-3.698	-1.609	3.205	0.131	2.5913
Sofosbuvir	64.308	-4.343	-1.873	1.023	-0.106	1.6565

Table 15. The correlation coefficient value (R^2) determined between Revan indices and the pharmacokinetic characteristics values of Zika virus drugs.

Revan indices	Intestinal absorption	CNS permeability	BBB permeability	Minnow Toxicity	Total clearance	LogP
R_1	0.558	0.556	0.530	0.098	0.253	0.034
HR_1	0.711	0.672	0.513	0.219	0.206	0.043
` SR	0.766	0.170	0.262	0.764	0.318	0.525
${}^mR_1$	0.886	0.339	0.363	0.756	0.087	0.823
R_2	0.759	0.708	0.509	0.286	0.195	0.082
HR_2	0.684	0.824	0.462	0.599	0.209	0.356
PR	0.891	0.361	0.322	0.767	0.140	0.825
${}^mR_2$	0.964	0.807	0.730	0.393	0.124	0.599

Revan indices	Intestinal absorption	CNS permeability	BBB permeability	Minnow Toxicity	Total clearance	LogP
FR	0.659	0.633	0.517	0.171	0.226	0.024
ABCR	0.825	0.500	0.655	0.551	0.460	0.397
GAR	0.890	0.434	0.575	0.720	0.298	0.477
HR	0.886	0.339	0.363	0.756	0.087	0.823
SDR	0.966	0.808	0.697	0.759	0.479	0.798

Table 16. The statistical parameters for the cubic regression model having the highest correlation coefficient value (R^2) for various Revan indices with physicochemical properties of Zika virus drugs.

Cubic model	R	F	S. E	P
IA=3.5E2+12.83 (SDR)-0.12$(SDR)^2$+3.31E-4$(SDR)^3$	0.983	37.373	5.308	0.002
CNS=-5+0.01(HR_2)-1.37E-5$(HR_2)^2$ + 2.39E-9$(HR_2)^3$	0.908	11.729	0.538	0.013
MT=43.66-5.55(PR)+0.23$(PR)^2$-3.01E-3$(PR)^3$	0.876	8.238	0.827	0.026
LogP= -50.2+6.29(PR)-0.24$(PR)^2$+2.82E-3$(PR)^3$	0.908	11.765	1.273	0.013

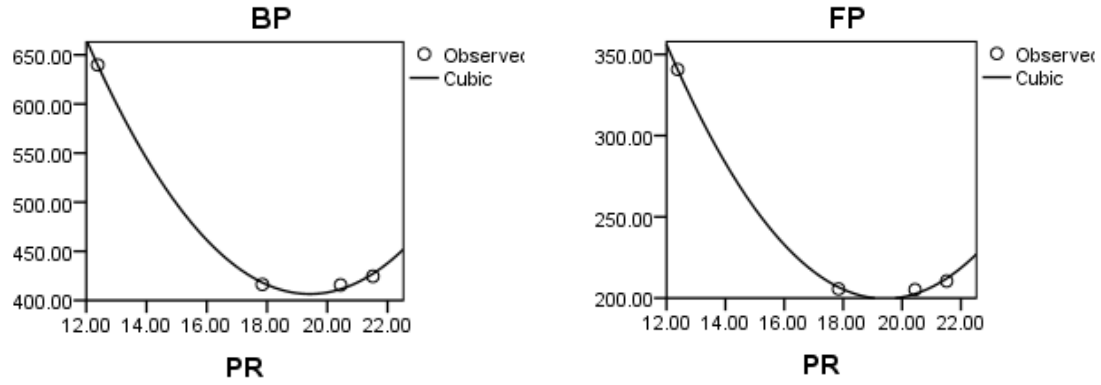

Figure 10. Cubic regression curves for PR index against BP and FP.

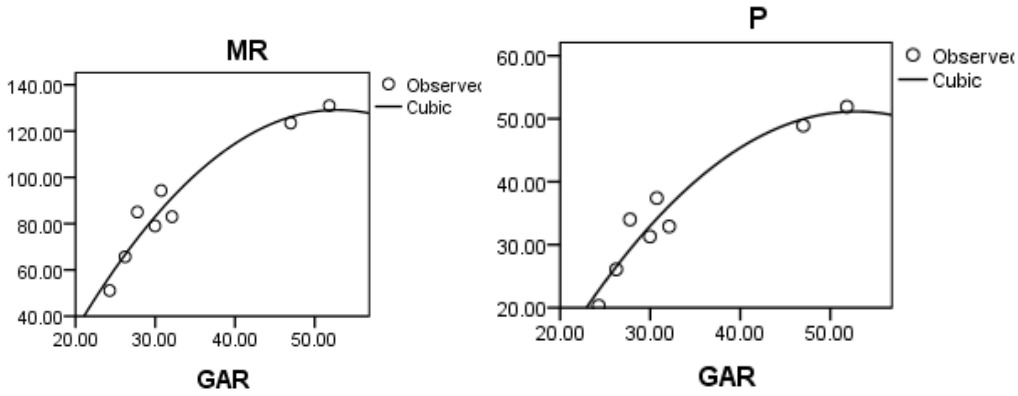

Figure 11. Cubic regression curves for GAR index against MR and P.

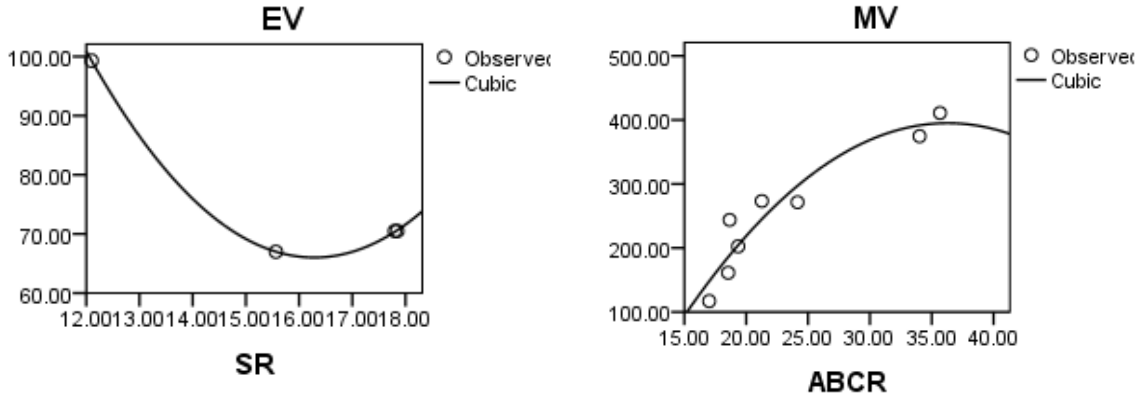

Figure 12: Cubic regression curve for SR index against EV and ABCR index against MV.

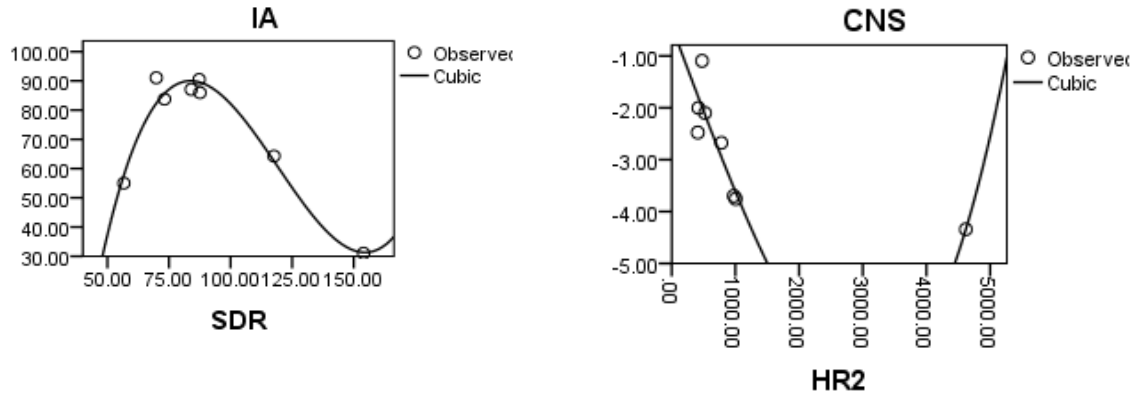

Figure 13. Cubic regression curve for SDR index against IA and HR_2 index against CNS.

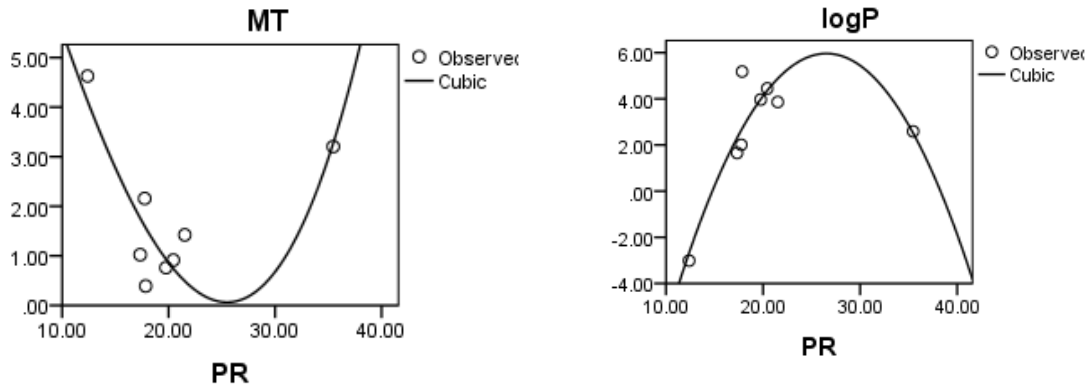

Figure 14. Cubic regression curve for PR index against MT and LogP.

The Revan indices that work well in cubic regression models for predicting the physicochemical and pharmacokinetic characteristics of Zika virus drugs include

Sum connectivity Revan index (*SR*) for predicting the boiling point (BP), Enthalpy of Vaporization (EV), and flash point (FP).

Product connectivity Revan index (*PR*) for predicting the boiling point (BP) and flash point (FP).

Second Hyper Revan indices (HR_2) for predicting the enthalpy of vaporization (EV).

Geometric-Arithmetic Revan index (*GAR*) for predicting the molar refraction (MR) and polarizability (P).

Atom-Bond connectivity Revan index (*ABCR*) for predicting the molar volume (MV).

Product connectivity Revan index (*PR*) for predicting the Minnow toxicity (MT) and LogP.

Symmetric Division Revan index (*SDR*) for predicting the intestinal absorption (IA).

Second Hyper Revan indices (HR_2) for predicting the CNS permeability (CNS).

4. Conclusions

The study of topological indices on the chemical structures of drugs can provide a theoretical foundation for drugs and chemical material synthesis. This paper's physicochemical and ADMET characteristics of several anti-flaviviral medicines were quantitatively analyzed using various Revan indices. The study reveals that chemists and the pharmaceutical industry may predict the characteristics of Zika virus therapies using theoretical analysis rather than time-consuming laboratory experiments. Further in this study, the correlation coefficient for different Revan indices was computed, enabling chemists to design novel drugs based on the

combination of positively highly correlated drugs. A similar study can be done on newly found drugs for a particular disease. A number of topological indices can be computed to estimate new drugs' physical and chemical characteristics.

Funding

This research received no external funding.

Acknowledgments

This research has no acknowledgments.

Conflicts of Interest

The authors declare no conflict of interest.

References

1. Aborode, A.T.; Sukaina, M.; Kumar, H. *et al.* Zika virus endemic challenges during COVID-19 pandemic in Africa. *Trop Med Health* **2021**, *49*, https://doi.org/10.1186/s41182-021-00372-6.
2. Charniga, K.; Cucunubá, Z.M.; Walteros, D.M.; Mercado, M.; Prieto, F.; Ospina, M.; *et al.* Descriptive analysis of surveillance data for Zika virus disease and Zika virus-associated neurological complications in Colombia, 2015–2017. *PLoS ONE* **2021**, *16*, e0252236, https://doi.org/10.1371/journal.pone.0252236.
3. Devillers, J. Repurposing drugs for use against Zika virus infection. *SAR and QSAR in Environmental Research* **2018**, *29*, 103-115, https://doi.org/10.1080/1062936X.2017.1411642.
4. Wiener, H. Structural determination of paraffin boiling point. *J. American Chemistry Society* **1947,** *69*,17-20, https://doi.org/10.1021/ja01193a005
5. Gutman, I.; Trinajstić, N. Graph theory and molecular orbitals. Total φ-electron energy of alternant hydrocarbons. *Chem. Phys. Lett* **1972**, *17*, 535-538, https://doi.org/10.1016/0009-2614(72)85099-1.
6. Estrada, E. Characterization of 3D Molecular structure. *Chemical Physics Letters* **2000**, *319*, 713-718. https://doi.org/10.1016/S0009-2614(00)00158-5
7. Havare, O. C. Topological indices and QSPR modeling of some novel drugs in the cancer treatment. *Int J Quantum Chemistry*, **2021**, *121*, e26813, https://doi.org/10.1002/qua.26813.
8. Jian- Feng Zhong; Abdul Rauf; Muhammad Naeem; Jafer Rahman; Adnan Aslam. Quantitative structure-property relationship (QSPR) of valency based topological indices with Covid-19 drugs and application. *Arabian Journal of Chemistry* **2021**, *14*, 103240, https://doi.org/10.1016/j.arabjc.2021.103240.
9. Kirmani, S. A. K.; Ali, P.; and Azam, F. Topological indices and QSPR/QSAR analysis of some antiviral drugs investigated for the treatment of COVID-19 patients. *Journal of Quantum Chemistry* **2021,** *121*, e26594, https://doi.org/10.1002/qua.26594.
10. Shanmukha, M.C.; Basavarajappa, N. S.; Shilpa, K. C.; Usha, A. Degree-based Topological indices in anticancer drugs with QSPR analysis. *Heliyon* **2020**, *6*, e04754, https://doi.org/10.1016/j.heliyon.2020.e04235.
11. Syed Ajaz, K.; Kirmani; Parvez Ali; Faizul Azam; and Parvez Ahmad Alvi. On Ve-Degree and Ev- Degree topological properties of Hyaluronic Acid- Anticancer drug conjugates with QSPR. *Journal of Chemistry* **2021**, *2021*, https://doi.org/10.1155/2021/3860856.
12. Syed Ahtsham UI Haq Bokhary; Adnan; Muhammad Kamran Siddiqui; and Murat Cancan. On topological indices and QSPR analysis of drugs used for the treatment of Breast cancer. *Polycyclic Aromatic Compounds*, **2021,** 6233-6253**,** https://doi.org/10.1080/10406638.2021.1977353.
13. 13. Sumiya Nasir; Nadeem, U.L.; Hassan Awan; Fozia Bashir Farooq and Saima Parveen. Topological indices of novel drugs used in blood cancer treatment and its QSPR modeling. *AIMS Mathematics* **2022**, *7*, 11829-11850, https://doi.org/10.3934/math.2022660.
14. Sourav Mondal; Arindam Dey; Nilanjan De; Anita Pal. QSPR analysis of some novel neighbourhood degree-based topological descriptors. *Complex and Intelligent Systems* **2021**, *7*, 977-996, https://doi.org/10.1007/s40747-020-00262-0.

15. Ozge Colakoglu. QSPR Modeling with Topological Indices of Some Potential Drug Candidates against COVID-19. *Journal of Mathematics* **2022,** *2022*, 1-9, https://doi.org/10.1155/2022/3785932.
16. Parvez Ali; Syed Ajaz , K.; Kirmani; Alok Kumar. Computation of Reverse Degrees of Some Antiviral Drugs Targeting COVID-19 with QSPR Analysis. *Biointerface Rresearch in Apllied Chemistry* **2023**, *13*, https://doi.org/10.33263/BRIAC131.066. .
17. Saima Parveen; Fozia ashir Farooq. Nadeem UL Hassan Awan, Rakotondrajao Fanja and Muhammad Farooq Choodhary, Topological indices of Drugs Used in Rheumatoid Arthritis Treatment and its QSPR Modeling. *Journal of Mathematics* **2022**, *2022*,1- 11, https://doi.org/10.1155/2022/1562125.
18. Tamilarasi, C.; Simon Raj, F. QSPR Analysis of Novel Indices with Priority Polycyclic Aromatic Hydrocarbons (PAHs). *Turkish Journal of Computer and Mathematics Education* **2021**, *12*, 3992-3999, https://doi.org/10.17762/turcomat.v12i10.5110.
19. Neha Kansal; Pravin Garg and Omendra Singh. Temperature – Based Topological Indices and QSPR Analysis of COVID-19 Drugs. *Polycyclic Aromatic Compounds* **2022,** https://doi.org/10.1080/10406638.2022.2086271.
20. Liu, J.B.; Arockiaraj, M.; Arulperumjothi, M.; and Prabhu, S. Distance based and bond additive topological indices of certain repurposed antiviral drug compounds tested for treating COVID-19. *Int. J. Quantum Chem* **2021,** *121*, 121, https://doi.org/10.1002/qua.26617.
21. Wei, J.; Cancan, M.; Rehman, A.U.;*et al*. On topological indices of remdesivir compound used in treatment of Corona virus (COVID-19). *Polycyclic Aromatic Compounds* **2021,** *45*, 1-19, https://doi.org/10.1080/10406638.2021.1887299.
22. Ravi, V.; Siddiqui, M.K.; Chidambaram, N.; and Desikan, K. On topological descriptors and curvilinear regression analysis of antiviral drugs used in COVID-19 treatment. *Polycyclic Aromatic Compounds* **2021,** *54*, 1-14, https://www.tandfonline.com/doi/abs/10.1080/10406638.2021.1993941.
23. Yang, J.; Muhammad, M.H. Siddiqui, M.k.; *et al*. Topological coindices of Hydroxyethyl starch conjugated with hydroxychloroquine used for COVID-19 treatment. *Polycyclic Aromatic Compounds* **2021,** *43*, 1-13, https://doi.org/10.1080/10406638.2021.1996407.
24. Rao Yongsheng; Kanwal Ammarah; Abbas Riffat; Noureen Saima; Fahad Asfand; Muhammad Imran Qureshi. Some degree-based topological indices of caboxy-terminated dendritic macromolecule. *Main Group Metal Chemistry* **2021**, *44*, 165-172, https://doi.org/10.1515/mgmc-2021-0016.
25. Kulli, V. R. Revan indices of oxide and honeycomb networks. *International Journal of Mathematics and its Applications* **2017**, *5*, 663-667.
26. Tamilarasi, W.; Balamurugan, B. J. ADMET and quantitative structure property relationship analysis of anti-Covid drugs against omicron variant with some degree-based topological indices. *Int. J. Quantum Chem.* **2022**, *122*, e26967, https://doi.org/10.1002/qua.26967.
27. Havare, O. C. Quantitative structure analysis of some molecules in drugs used in the treatment of COVID-19 with topological indices. *Polycyclic Aromatic Compounds* **2021,** *42***,** https://doi.org/10.1080/10406638.2021.1934045.
28. Kulli, V. R.; Hyper Revan indices and their polynomials of silicate network. *International Journal of Current Research in Science and Technology*, **2018,** *4*, 17-21.
29. Kulli, V. R. Computing the F-Revan and modified Revan indices of certain nanostructures. *J. Comp. and Math. Sci.* **2018,** *9*, 1326-1333, http://dx.doi.org/10.29055/jcms/875.
30. Kulli, V. R. The sum connectivity Revan index of silicate and hexagonal networks. *Annals of Pure and Applied Mathematics* **2017,** *14*, 401-406, http://dx.doi.org/10.22457/apam.v14n3a6.
31. Kulli, V. R. On the product connectivity Revan index of certain nanotubes. *Journal of Computer and Mathematical Sciences* **2017,** *8*, 562-567, http://dx.doi.org/10.29055/jcms/694.
32. Kulli V. R. F-Revan index and R-Revan polynomial of some families of benzenoid systems. *Journal of Global Research in mathematical Archives* **2018,** *5*, 1-6.
33. Kulli V. R. Revan indices of Chloroquine, Hydroxychloroquine, Remdesivir: Research advances for the treatment of COVID-19. *International Journal of Engineering Sciences and Research Technology* **2020,** *9.*